Electrical properties of sprayed CuInS$_2$ films for solar cells

A. Mere[*], O. Kijatkina, H. Rebane, J. Krustok, M. Krunks

Institute of Materials Science, Tallinn Technical University, Ehitajate tee 5, Tallinn 19086, Estonia

Abstract

CuInS$_2$ films and superstrate configuration ZnO/CdS/CuInS$_2$ solar cells were prepared by cost-effective spray pyrolysis technique using the Cu/In molar ratios of 0.9, 1.0 and 1.1 in spray solution. Appropriate metal chlorides and thiourea were used as starting chemicals to prepare the absorber layer. XRD, scanning electron microscopy, current–voltage, capacitance–voltage and frequency-swept admittance spectroscopy methods have been used to characterize sprayed absorber and solar cell. It has been shown that the carrier concentrations in CuInS$_2$ absorber layer is close to 10^{17} cm^{-3} and V_{OC} temperature dependent curve extrapolated to $T = 0$ K gives $V_{OC}(0)$ of 1.06 V. The columnar microstructure and small size of crystallites in sprayed films supposed to be responsible for inferior output characteristics of sprayed solar cell as $V_{OC} = 443$ mV, $j_{SC} = 5.5$ mA cm^{-2}, FF = 37%. According to the frequency-swept capacitance measurements the junction with lowest energy losses is formed with the absorber deposited from In-rich solution.
© 2003 Elsevier Ltd. All rights reserved.

Keywords: A. Chalcogenides; A. Thin films; A. Multilayers; B. Chemical synthesis; D. Electrical properties

1. Introduction

Solar cell efficiencies of 11.4% are achieved on CuInS$_2$ based thin film PV cells using vacuum-based preparation technique [1,2]. The up scaling of vacuum-based technologies is believed effectively to reduce the costs to the level acceptable for the terrestrial applications [3]. The alternative approach is the implementation of low-cost thin film deposition techniques and principally different solar cell design. During the last years the studies on the superstrate configuration cells [4] and low-cost thin film deposition methods as chemical bath deposition, chemical spray pyrolysis and electrodeposition have been intensively studied.

In the present study, CuInS$_2$ absorber layers and superstrate configuration solar cells are prepared by a cost-effective spray pyrolysis technique. The effect of the deposition conditions as the growth temperature and the molar ratio of the precursors in the initial solution on the structural and optical properties, phase and elemental composition of sprayed chalcopyrite films has been properly studied [5–8]. There are only few studies which deal with

the electrical properties as resistivity and mobility of carriers in sprayed films [9,10].

In the present study, both sprayed CuInS$_2$ absorber layers and corresponding solar cells are characterised with respect their electrical and structural properties depending on the Cu/In molar ratio in spray solution.

2. Experimental

Superstrate configuration solar cell structures ZnO/In,ZnO/CdS/CuInS$_2$ were prepared using the spray process for all layers. Indium tin oxide (ITO) coated glasses were used as substrates. ZnO layers were prepared from Zn(CH$_3$CO$_2$)$_2$·2H$_2$O. Thin CdS buffer layer was deposited using an aqueous solution of CdCl$_2$ and SC(NH$_2$)$_2$. The deposition processes of ZnO and CdS layers are described in detail in Ref. [11]. CuInS$_2$ absorber was deposited by spray of an aqueous solution of CuCl$_2$, InCl$_3$ and SC(NH$_2$)$_2$ onto ITO coated glass substrates and on the top of ZnO/In,ZnO/CdS structure at 370 °C. The absorber layers with similar thickness of 500 nm were grown from the solutions using the molar ratios of precursors Cu/In = 0.9–1.1 and S/Cu = 3. The cell structure thickness was close to 1 μm. Sprayed absorbers were etched in an aqueous solution of

* Corresponding author. Fax: +372-6202020.
E-mail address: amere@edu.ttu.ee (A. Mere).

Table 1
Carrier concentrations as determined by C–V measurements, Cu/In as determined by EDS in sprayed $CuInS_2$ films and characteristics of sprayed $ZnO/CdS/CuInS_2$ solar cells

Cu/In molar ratio		Solar cell						Schottky barrier
Solution	Film	Cell	V_{OC} (mV)	j_{SC} (mA cm^{-2})	FF	R_S (Ω)	N_p (cm^{-3})	N_p (cm^{-3})
0.90	0.98	A	336	0.26	0.27	3000	1.8×10^{17}	2.7×10^{17}
1.00	1.09	B	443	5.5	0.37	270	2.1×10^{17}	2.2×10^{17}
1.10	1.17	C	380	3.4	0.38	220	8.7×10^{16}	No barrier

KCN (5%) + KOH (0.5%) at room temperature. Conductive carbon paste was used as an electrode ($A = 1.5$ mm^2) to $CuInS_2$. Schottky barrier was prepared by evaporation of Al contact on the top of $CuInS_2$ films on ITO electrode.

Sprayed films and solar cells were examined by XRD using a Bruker AXS D5005 diffractometer with monochromatic Cu K$_\alpha$ radiation and scanning electron microscopy (SEM) using a Jeol JSM-840A. The thickness of the films and solar cell structures was determined from the SEM cross-sectional micrographs. Current–voltage (I–V), capacitance–voltage (C–V) and frequency-swept admittance spectroscopy measurements were performed using an AUTOLAB PGSTAT 30 set-up. Solar cell output characteristics were measured under a halogen lamp illumination with the intensity of 100 mW cm^{-2}. Open-circuit voltage (V_{OC}) versus temperature was measured by a Keithley digital electrometer (model 616) using liquid nitrogen cryostat to set the temperature.

3. Results

3.1. Concentration of carriers in sprayed $CuInS_2$ films and performance of sprayed solar cell

Sprayed $CuInS_2$ films were prepared using the Cu/In = 0.9–1.1 in spray solution as according to our previous studies, these conditions allow to get the films with smooth surface and their chemical composition is homogeneous over the deposited area [6]. The effect of the Cu/In in solution on the Cu/In in etched absorber film as measured by EDS over the surface area of 2×2 μm^2, is presented in Table 1. The results on the elemental composition are in accordance with previously published results indicating the loss of In during the spray process [6,12].

The films prepared under the chosen deposition conditions show p-type conductivity and optical bandgap close to 1.45 eV as it is shown in our previous studies [5,12]. In this part of the work, the carrier concentrations in sprayed films and the characteristics of sprayed solar cells will be presented.

Mott–Schottky model was applied to determine carrier concentrations in the films. C–V curves of

$CuInS_2$/Al Schottky barriers and $ZnO/CdS/CuInS_2$ solar cell structures were recorded in the region of voltages from -2 up to 0 V at 1 kHz. The carrier concentrations calculated from the slope of $1/C^2$ versus voltage plot are presented in Table 1. The carrier concentrations in sprayed absorber layer are on the level of 10^{17} cm^{-3} calculated from Schottky barrier or p–n junction using the Cu/In = 0.9–1.0. Accordingly, these films exhibit similar properties in top and bottom areas. The use of the Cu/In = 1.1 leads to the films where no Schottky barrier was formed if Al electrode was deposited on the top of the film. The deposition of absorber layer from Cu-rich solution onto CdS layer results p–n junction. The observed phenomenon probably refers onto different properties in bottom and top of sprayed $CuInS_2$ film.

The I–V characteristic of all layers sprayed $ZnO/CdS/CuInS_2$ cell using the Cu/In = 1 in solution is shown in Fig. 1. The cells output characteristics which depend on the Cu/In in solution are shown in Table 1.

The parametres of spray deposited solar cells are far from the values presented for the best $CuInS_2$ based cells. Low values of short circuit current density j_{SC}, especially in
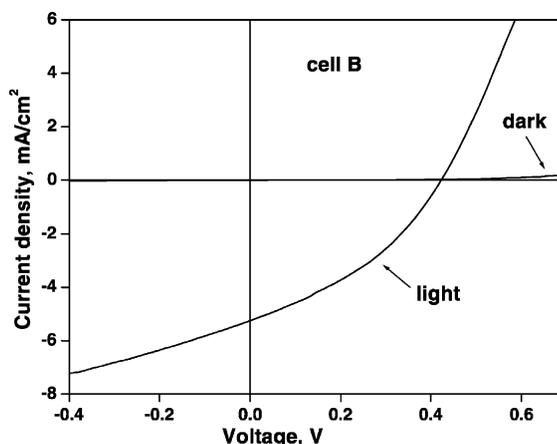

Fig. 1. I–V characteristics of sprayed $ZnO/CdS/CuInS_2$ solar cell in dark and under a halogen lamp illumination at intensity of 100 mW cm^{-2}. In Cell B the absorber layer was deposited from the solution with the Cu/In = 1.

the case of the absorber from In-rich solution (cell A), could be caused by high serial resistance R_S of the structure (Table 1). Serial resistances of the cells B and C are similar and result in quite similar short circuit current density values.

The section of the XRD patterns of sprayed cells in the region of $2\theta = 25–30°$, submitting the (112) peak of $CuInS_2$, is shown in Fig. 2. $CuInS_2$ film prepared from In-rich solution (cell A) show very broad diffraction peak. The increase in copper concentration in solution supports the increase in crystallite size (cells B and C). The XRD results on $CuInS_2$ in solar cell structure are in good correspondence with the results reported earlier for spray deposited films on glass substrates [5–8]. Consequently, small crystallite size of the absorber deposited from In-rich solution could be one reason for the lowest j_{SC} compared with other sprayed cells. Additionally, SEM micrograph of the cross-section of sprayed $CuInS_2$ film on glass substrate (Fig. 3) shows columnar sparse microstructure and therefore p–n junction area may be smaller than expected and used for the current density calculations.

The dependence of V_{OC} on the temperature has been measured for solar cells (Fig. 4). The plot of V_{OC} vs. temperature T, extrapolated to $T = 0$ K gives $V_{OC}(0)$ characterising the barrier height of the junction. Cell B, prepared from the solution with the Cu/In $= 1$, shows the highest $V_{OC}(0) = 1.06$ V which is close to that reported for $CuInS_2$-based solar cells prepared by the other techniques [1,13]. Low values of $V_{OC}(0) \approx 1.0$ V could be induced due to the interface recombination [13].

3.2. Frequency-swept admittance spectroscopy measurements

Frequency-swept admittance measurements were carried out for zero and 2 V DC reverse biased solar cell
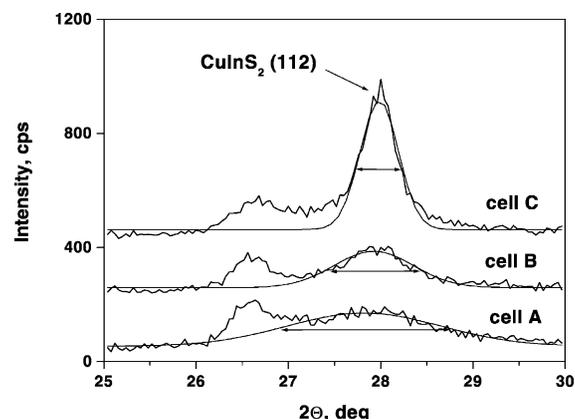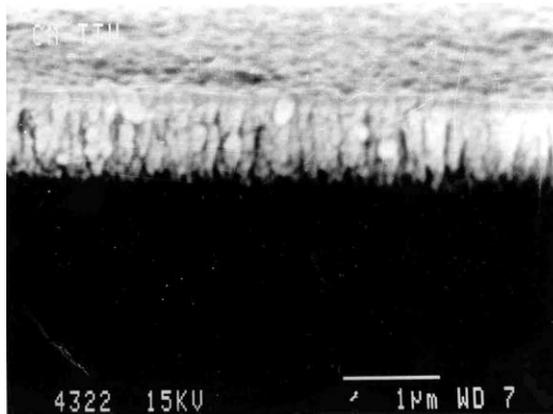

Fig. 3. SEM micrograph of the cross-section of spray deposited $CuInS_2$ film on glass substrate using the molar ratio of Cu/In $= 1$ in solution.

structures in the frequency range of $10–10^6$ Hz at room temperature in dark. AC voltage of 10 mV RMS was applied on the junction. The capacitance of the cells was calculated from admittance data assuming parallel RC equivalent circuit.

The junction capacitance of the cells per unit area versus frequency at two different biases is shown in Fig. 5. All investigated solar cell structures reveal the frequency dependent capacitance. Our cells could be divided into two groups according to the capacitance–frequency characteristics. The first, where $C/A = f(F)$ curve shows two slopes, is characteristic for cell A. Capacitance is almost independent of the frequency in the interval of $10^4–10^6$ Hz and a frequency dependent part appears at frequencies lower than 10^4 Hz. The second set of curves where large

Fig. 2. The section of the XRD patterns of sprayed ZnO/CdS/CuInS$_2$ cells using different Cu/In molar ratios in spray solution to deposit CuInS$_2$: Cell A—Cu/In $= 0.9$, Cell B—Cu/In $= 1$, Cell C—Cu/In $= 1.1$.
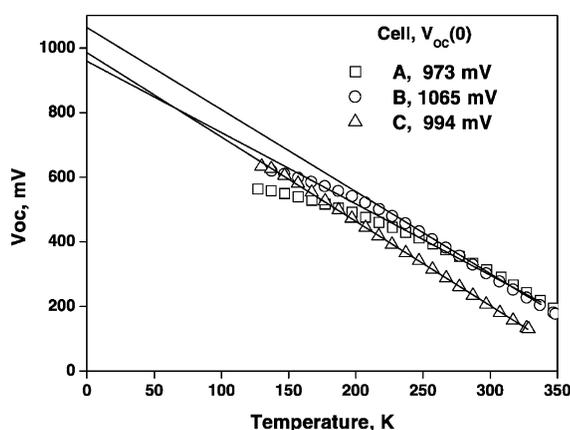

Fig. 4. V_{OC} of solar cells versus temperature. Labelling of the cells corresponds to that shown in Fig. 2. Corresponding V_{OC} values at 0 K are presented.
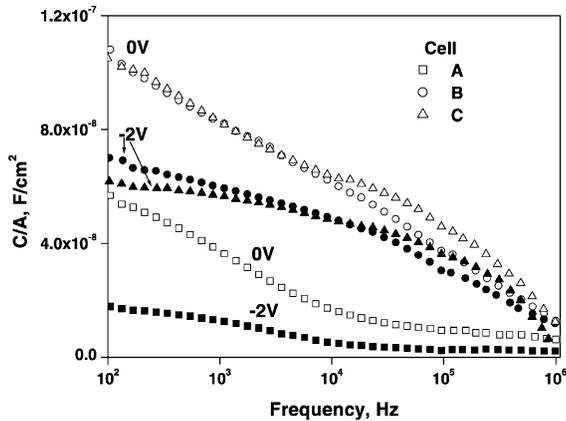
Fig. 5. Capacitance per unit area versus frequency for solar cells at two different biases. Labelling of the cells corresponds to that shown in Figs. 2 and 4.

capacitance dispersion over all the frequency range is observed (cells B and C) is similar to those recorded for sprayed CuInSe$_2$/CdS solar cells [14].

Energy loss tangent as a merit of energy losses in the circuit [15] has been used to characterise the prepared cells. The energy loss tangent is determined as

$$\tan \delta = \frac{Z''}{Z'},$$

where Z' is the real and Z'' is the imaginary part of the impedance.

The loss tangent curve of cell A clearly shows two peaks (Fig. 6). The peak close to 130 Hz at zero bias shifts to the higher frequency of 270 Hz when the scan was made at reverse bias of 2 V. The observed feature is the evidence of the losses in space charge region. The peak at
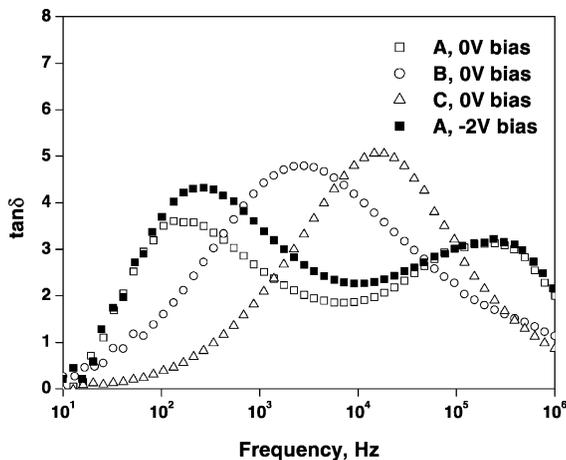
3×10^5 Hz is independent of the bias. Consequently, the second loss tangent peak is not raised from the junction and could be caused by the contacts or grain boundaries. The similar effect appears in smaller extent in cell B and is negligible in cell C. The observed effect supports the speculation that the bias independent peak could be caused by the grain boundaries as the main difference between cells A and C consists in absorbers with strikingly different crystallite size proved by the XRD (Fig. 2).

The loss tangent value of bias-dependent peaks (at zero biasing) increases and the peak position shifts to higher frequencies from cell A to C (Fig. 6). Therefore, the electrical losses in space charge region of cell A are lower than that in cells B and C. Further research is needed to discuss the observed loss tangent peak shift.

4. Conclusions

CuInS$_2$ absorber layers with carrier concentrations close to 10^{17} cm^{-3} could be prepared by spray pyrolysis method using the Cu/In = 0.9–1.1 in solution as determined by C–V measurements. The carrier concentration in absorber and the V_{OC} of all components sprayed ZnO/CdS/CuInS$_2$ solar cells at 0 K of 1.0 V are similar to that reported for CuInS$_2$-based cells made by the other techniques.

The columnar microstructure and small size of crystallites in sprayed films, confirmed by SEM and XRD, could be responsible for low output characteristics of sprayed cells. Additionally, columnar microstructure offers favoured conditions for short circuiting.

The development of solar cells by cost-effective spray technique requires the preparation conditions resulting in dense absorber layers with larger crystallites using preferably In-rich spray solution.

Fig. 6. Energy loss tangent versus frequency for solar cells at zero (cells A–C) and −2 V (cell A) biases. Labelling of the cells corresponds to that shown in Figs. 2, 4 and 5.

References

[1] S. Siebentritt, Thin Solid Films 403–404 (2002) 1.
[2] M. Powalla, B. Dimmler, Solar Energy Mater. Solar Cells 76 (2001) 337.
[3] M.R. Balboul, A. Janesek, O. Chernykh, U. Rau, H.W. Schock, Thin Solid Films 387 (2001) 74.
[4] K. Siemer, J. Klaer, I. Luck, J. Bruns, R. Klenk, D. Bräunig, Solar Energy Mater. Solar Cells 67 (2001) 159.
[5] M. Krunks, O. Bijakina, T. Varema, V. Mikli, E. Mellikov, Thin Solid Films 338 (1999) 125.

[6] M. Krunks, V. Mikli, O. Bijakina, H. Rebane, A. Mere, T. Varema, E. Mellikov, Thin Solid Films 361–362 (2000) 61.

[7] S. Shirakata, T. Murakami, T. Kariya, S. Isomura, Jpn. J. Appl. Phys. 35 (1996) 191.

[8] M.C. Zougi, T. Ben Nasvallah, S. Marsillac, J.C. Bernede, S. Belgacem, Thin Solid Films 382 (2001) 39.

[9] H. Bozouita, N. Bouguila, A. Dhouib, Renewable Energy 17 (1999) 85.

[10] H. Bihri, C. Messaoudi, D. Sayah, A. Boyer, A. Mzerd, A. Abd-Lefdil, Phys. Stat. Sol (a) 129 (1992) 193.

[11] O. Kijatkina, M. Krunks, A. Mere, B. Mahrov, L. Dloczik, Thin Solid Films (2003) in press.

[12] M. Krunks, O. Bijakina, V. Mikli, H. Rebane, T. Varema, M. Altosaar, E. Mellikov, Solar Cell Mater. Solar Cells 69 (1) (2001) 93.

[13] M. Turcu, O. Pakma, U. Rau, Appl. Phys. Lett. 80 (2002) 2598.

[14] W.A. Stifler, C.W. Bates, J. Appl. Phys. 71 (1992) 4358.

[15] P. Stallinga, H.L. Gomes, H. Rost, A.B. Holmes, M.G. Harrison, R.H. Friend, F. Biscarini, C. Taliani, G.W. Jones, D.M. Taylor, Physica B 273–274 (1999) 923.